ISSN 2007-9737

Indirect Monitoring Cane Sugar Crystallization via Image Fractal Analysis

Armando Campos-Dominguez[1,2], Yessica I. Ceballos-Ceballos[3], Sergio A. Zamora-Castro[4], Eliseo Hernandez-Martinez[3], Oscar Velazquez-Camilo[4,5]

[1] Universidad Veracruzana,
Facultad de Ingeniería Mecánica y Eléctrica,
Mexico

[2] Universidad Veracruzana,
Facultad de Ingeniería Eléctrica y Electrónica,
Mexico

[3] Universidad Veracruzana,
Facultad de Ciencias Químicas, Región Xalapa,
Mexico

[4] Universidad Veracruzana,
Facultad de Ingeniería de la Construcción y el Hábitat,
México

[5] Universidad Veracruzana, Región Veracruz,
Facultad de Ciencias Químicas,
Mexico

{acampos, szamora, elisehernandez, ovelazquez}@uv.mx, yessica_yicc@hotmail.com

Abstract. Due to the increasing demands of quality products, efficient monitoring systems in the current control and operation of industrial processes are essentials. However, in particulate processes as cane sugar crystallization, accurate, inexpensive and suitable sensors for the online monitoring of key process variables are not available. In this work, an alternative using the image analysis of micrographs captured in batch cooling crystallizer is presented. The propose is based on a combined treatment between fractal analysis and conventional binarization techniques, obtaining a normalized fractal index (*NFI*) that allow the dynamic monitoring of crystal mean diameter, *D(4,3).* In order to evaluate the monitoring system, the crystallizer was operated at different cooling profiles, finding that the methodology proposed can be used as an alternative technique, inexpensive and easy to implement, for monitoring crystal growth.

Keywords. Cane sugar crystallization, monitoring crystal growth, image fractal analysis.

1 Introduction

Monitoring and control of the crystallization process is of great interest in different chemical industries as pharmaceutical, food production industries, among others. Particularly, the cane sugar production is one of the most important industrial processes around the globe. The cane sugar crystallization is a solid-liquid separation, where the solute in a liquid phase is transferred to a solid phase, which leads to crystal formation. The quality of the final product is determined by the size and shape of the crystals.

Therefore, monitoring and control of crystallizers is one of the biggest challenges the sugar industry faces. For this reason, extensive studies have focused on the design of strategies to control the crystallization process, including the

development of mathematical models [3, 12, 15, 19].

For instance, Bohlin and Rasmuson [12] proposed a general mathematical model to describe crystals size growth, and through numerical simulations determined that the cooling profile control is not enough to control of crystal size. This is due to the complex kinetics of crystal growth, which is affected by different factors, such as pressure and agitation. Later on, Tahal [19] proposed a more complex model, which considered the dispersion of the crystal growth rate in a vacuum batch crystallizer. Experimental data was used to the parameter adjustment, allowing the prediction of crystals size growth rate. In addition, by means of numerical simulations, they proposed the implementation of a PID feedback controller.

Furthermore, Quintana et al., [15] proposed a dynamic model to estimate the kinetic parameters of the sugarcane crystallization process. An agitation velocities range (50 to 600 min^{-1}) and different cooling profiles (step, negative exponential, linear and cubic) were considered to evaluate the sugar crystals growth, finding that the effects these parameters have over size and crystals distribution. Recently, considering a population balance model Damour et al. [3, 4] proposed a multivariable control scheme for monitoring crystals concentration. The controller is adapted to a state observer, which allows estimating the uncertain model parameters.

Their results were complemented using industrial data, ensuring that the controller allows the concentration monitoring, even under external disturbance. Despite these results, the practical application of mathematical models is limited since they do not describe in detail the existing transport phenomena interactions. Therefore, it is not possible to precisely predict the growth and crystals size distribution.

Thus, in the last years, monitoring crystals growth by means of captured images analysis during the process (i.e., straight from the sugar crystals solution with uncrystallized mixture) has increased, allowing visually identify the dynamic advance of the crystals size.

In this sense, De Anda et al. [9] reported the image acquisition using high-speed cameras and electronic microscopes can be coupled to a feedback controller for crystal size control.

Wang et al. [21] performed the measurement of growth rates of β L-glutamic acid crystals using image techniques and on-line analysis in a batch crystallization. Afterwards, Velázquez-Camilo et al. [13] proposed the application of detrended fluctuation analysis (DFA) to study patterns in cane sugar crystals growth related to crystal mean diameter (*D(4,3)*); their results showed that the mass fractal dimension (D_f) exhibits positive correlations with *D(4,3),* which can be used for monitoring of crystals growth. Moreover, Velázquez-Camilo et al. [14] analyzed the lacunarity index in sugarcane micrographs identifying patterns that allow quantifying the crystal mass formed (*CMF*). On the other hand, Zhang et al. [2] employed the wavelet transform to analyze images of NaCl crystals finding patterns to the evaluation the crystal distribution during the process.

Previous results show that the image analysis is a potential tool for monitoring of crystals growth. However, the methodologies have not been standardized, also they not have been assessed at different crystallizer operating conditions. Then, in this paper an unconventional image analysis for monitoring sugar-cane crystal growth in a crystallizer batch (pilot plant scale), operated to different cooling temperature profiles is proposed.

Image analysis methodology considers information obtained by image processing using binarization and fractal analysis. In order to evaluate the fractal descriptor performance for crystals monitoring, experimental tests were carried out under various operation conditions of the process. The results indicate that the fractal descriptor provides useful information for the monitoring of crystals growth through direct correlation between the fractal index and *D(4,3).*

2 Experimental Setup

In this section, the equipment and experimental operational conditions for sugarcane crystallization is described.

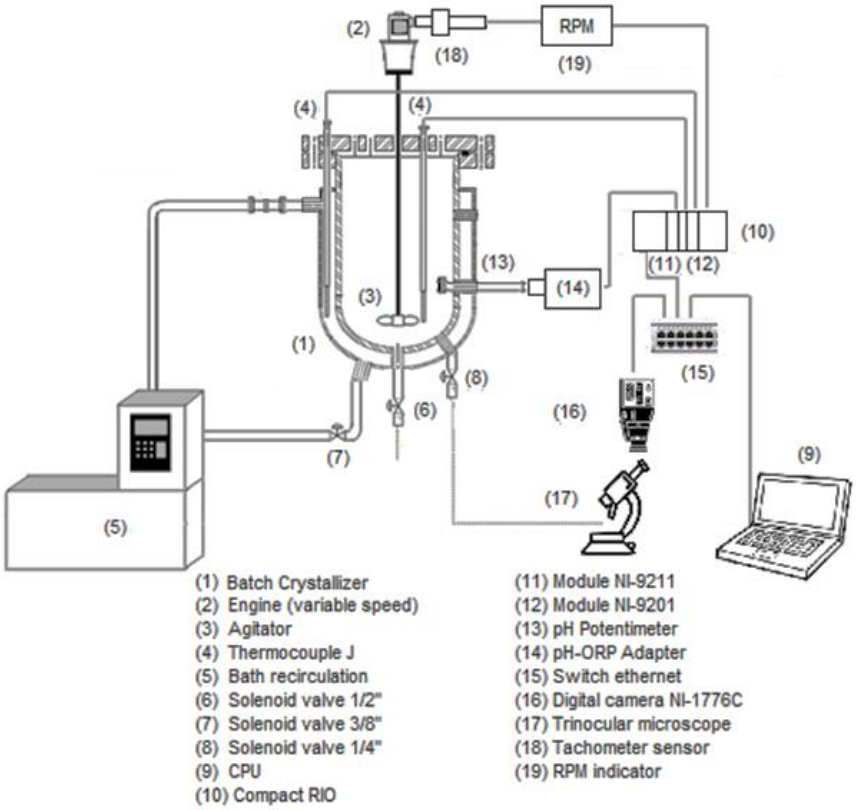

Fig. 1. Experimental set-up of batch crystallizer at pilot plant scale and data acquisition system

2.1 Batch Crystallizer

The experimental tests were performed in a stainless steel batch crystallizer (9.2 L) with heating-cooling jacket (4.8 L) at pilot plant scale (see Figure 1).

The agitation engine can be adjusted at variable speed, include an optical sensor with a digital tachometer. The micrographs were obtained using a trinocular Cole-Parmer microscope with digital camera integrated (National Instruments Inc.). A Supervisory Control and Data Acquisition interface was developed in LabVIEW software.

2.2 Saturated Solution

The saturated solution for sugarcane crystallization was prepared at 70 °C, according to the solubility data obtained experimentally by Bolaños-Reynoso [5]:

$$C_{70°C} = \frac{°Brix_{theoretical}}{100 - °Brix_{theoretical}}, \quad (1)$$

where °*Brix* is obtained by:

$$°\text{Brix} = 0.0005\ T^2 + 0.1566\ T + 63.021. \quad (2)$$

2.3 Operation Conditions

First, the solution is heated at 70 °C, where it is seeded 1.85 g of crystal nucleus of 150 μm average size. The agitation speed is adjusted to 250 min^{-1}. Each experiment lasted 240 min (from the seeding to the batch unloading), considering three cooling profiles described as follow:

– The natural temperature profile consists in cooling the solution from 70 °C to 40 °C, by

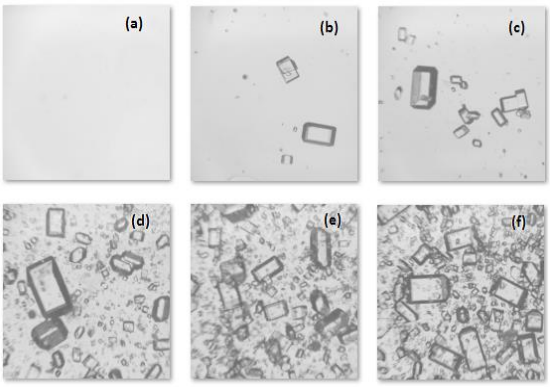

Fig. 2. Micrograph sequence of crystal growth using linear temperature profile, a) 0 min, b) 60 min, c) 105 min, d) 150 min, e) 195 min and f) 240 min

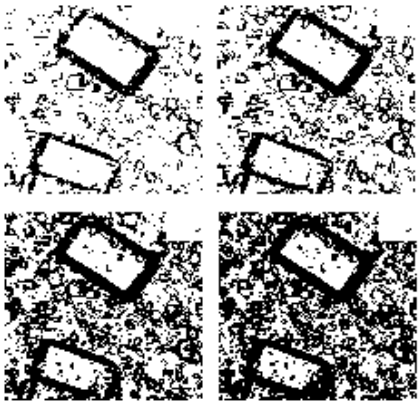

Fig. 3. Image binarization for linear temperature profile at *t*=150 min considering different threshold, a) 0.55, b) 0.65, c) 0.75, and d) 0.85

constantly providing cooling water at 40°C to the jacket during all the crystallization process.

– The lineal temperature profile leads from 70 °C to 40 °C by an indexed linear function (Eq. 3) during the operation time (240min):

$$T = -0.002083t + 70. \quad (3)$$

– The cubic temperature profile is guided by a cubic equation (Eq. 4). The drop-in temperature is slow requiring 4 hours to change from 70°C to 40°C:

$$T = -1\text{x}10^{-11}\, t^3 + 6.2\text{x}10^{-8}\, t^2 - 0.0009\, t + 70, \quad (4)$$

where T is the temperature crystallizer in °C and t is the process time in seconds. For each cooling temperature profile, the experiments were performed in triplicate.

2.4 Micrographs Acquisition

The micrographs acquisition is performed, taking saturated solution samples (5 mL) at 15 min intervals. For each sample four images were captured to image resolution of 1200x1200 pixels in a*.png format. In Figure 2, a micrograph sequence for the experimental test with linear cooling profile is shown.

Notice that crystals growth is not exhibited a regular pattern. Subsequently, the crystals are separated using a basket centrifuge at 4000 min^{-1} for 10 min. and dried in chamber with forced convection at 60 °C for 36 hours, so the *CMF* is obtained.

3 Image Processing

3.1 D(4,3) Determination

A standard parameter to determine crystal size is the crystal mean diameter, *D(4,3)*, which traditionally is obtained by the calculating of perimeter for each crystal in an image.

For this end, we used a Vision Assistant 2012 of National Instruments Inc. software. Once the perimeters are obtained, data is exported to the DTC Adq-Im Ver. 1.0 software where the *D(4,3)* and its corresponding standard deviation (*S(4,3)*) were determined [5].

3.2 Micrographs Binarization

The image binarization is a transformation of pixels to scale 0 and 1 for white and black colors, respectively. As an index of binarization, the pixel average (P_A) is calculated as:

$$P_A = 1 - \frac{1}{NM}\sum_{i=1}^{N}\sum_{j=1}^{M} A_{i,j}\ , \quad (5)$$

where A_{ij} are the pixel values. Consider the linear cooling profile, Figure 3 shows micrographs at t=150 min using different threshold intensities

(0.55, 0.65, 0.75, and 0.85), where for 65 % threshold the crystal contours in the image are highlighted.

3.3 Fractal Analysis

Image fractal analysis has been applied to a large diversity physical and chemical processes [1, 6, 7, 10, 13, 18, 21], providing useful correlations that contribute to the characterization of such processes. Range rescaled (*R/S*) analysis is one of the most traditional method in engineering process [8, 17, 20]. The description of the two-dimensional *R/S* method is described in [8]. So, for convenience in this work a brief description is also presented. First, it is necessary to transform the image to gray scale, assigning a numerical value to each pixel (i.e., 0 to 256).

This leads to a *NxM*-dimensional matrix. In order to analyze different scales, $s \in [\![0,1]\!]$ subsamples of $N_k x M_k$-dimensional ($N_k=sN$ and $M_k=sM$) are considered. Next, for each subsample the re-escalated range is computed as:

$$(R/S)_S = \frac{1}{\sigma_S}\left[\max_{\substack{1\le i\le N_k \\ 1\le j\le M_k}} \sum_{l=1}^{i}\sum_{n=1}^{j}(y_{l,n}-\bar{y}_S) - \min_{\substack{1\le i\le N_k \\ 1\le j\le M_k}} \sum_{l=1}^{i}\sum_{n=1}^{j}(y_{l,n}-\bar{y}_S)\right], \quad (6)$$

where $\bar{y}_S$ and σ_S are the average and standard deviation of the subsample, respectively, such as:

$$\bar{y}_S = \frac{1}{N_k M_k}\sum_{i=1}^{N_k}\sum_{j=1}^{M_k} y_{i,j}, \quad (7)$$

$$\sigma_S = \left[\frac{1}{N_k M_k}\sum_{i=1}^{N_k}\sum_{j=1}^{M_k}(y_{i,j}-y_S)^2\right]^{\frac{1}{2}}. \quad (8)$$

The re-scaled range must be calculated in a sufficiently large number of subsamples of different sizes s. For a certain domain $s \in (s_{\min}, s_{\max})$, the statistic *R/S* follows a power law, such as:

$$(R/S)_S = as^{2H}, \quad (9)$$

where *a* is a constant and *H* is the scaling Hurst exponent, which is a measurement of the fractal sequence correlations. A log-log graph (R/S) as a function of the scale squared, generates a line with slope *H*. The interpretation of the parameter *H* can be related to the roughness of the image surface by fractal dimension (D_f=3-*H*), where the closer *H* to 0, the rougher image and the closer *H* to 1, the smoother the corresponding texture [8].

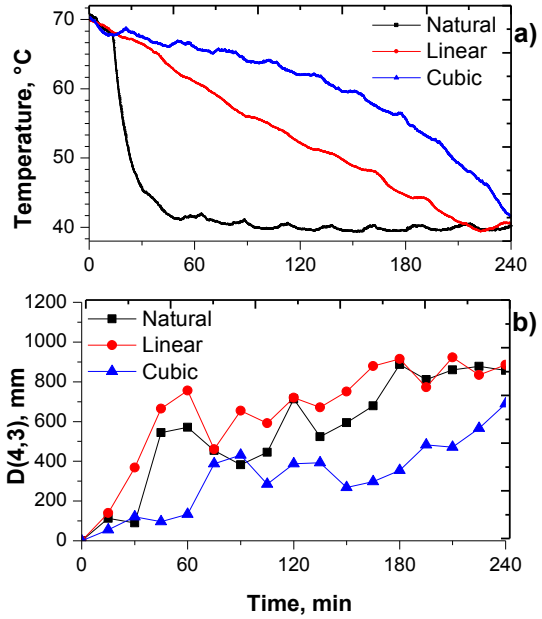

Fig. 4. a) Cooling temperature profiles, and b) *D(4,3)* calculate by Vision Assistant software

4 Results and Discussion

Figure 4a shows the proposed cooling profiles for the experimental development (i.e., natural, linear and cubic), where it can be observed that the natural profile reaches 40 °C in 120 min and it remains constant, whereas the linear and cubic profiles were programmed to reach 40 °C in 240 min. As expected, each temperature profile exhibits a different crystal growth. Consider four images for each sample, Figure 4b shows the average *D(4,3)* as a function of time, indicating that in steady state a larger value is reached for the linear profile with respect to the cubic profile. This result is consistent with that reported by Quintana-Hernandez et al. [6].

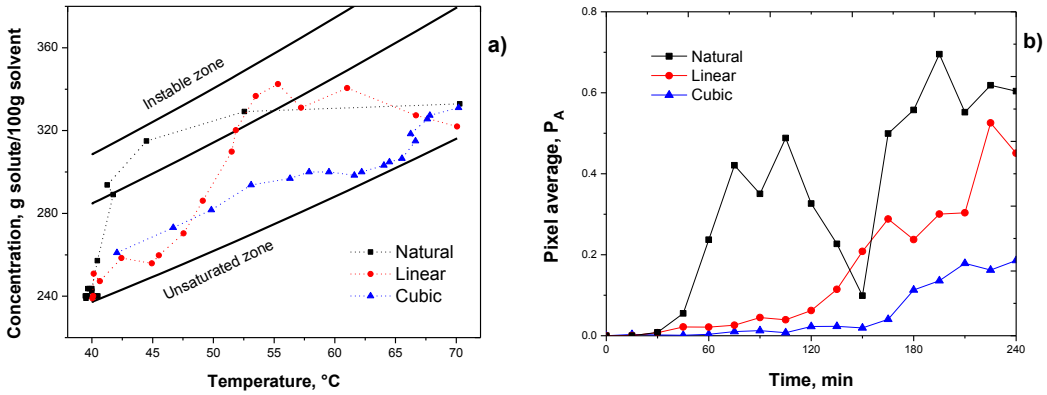

Fig. 5. a) Miers diagram for sugar cane crystallization process for three temperature profiles, and b) average binarized pixels for image sequences considering different operation conditions

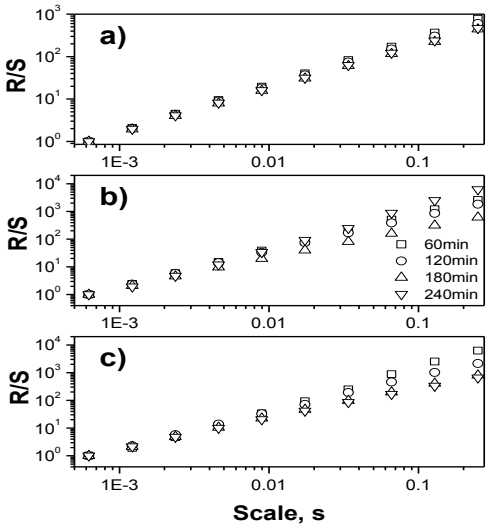

Fig. 6. *R/S* analysis for cane sugar images captured during crystallization process, a) linear, b) natural and c) cubic temperature profiles

Figure 5a shows the Miers diagram for sugarcane crystallization, where four zones can be identified: i) unstable zone; ii) first metastable zone or labile zone where the nucleation is the kinetic dominant; iii) second metastable zone where the crystal growth is the most important process; iv) unsaturated zone where is not possible the crystal formation.

Experimental data corresponding to Figure 5b is joined in Miers diagram supporting that linear profile exhibit greater crystal growth than cubic profile; also, it is observed that natural profile leads to nucleus formation, which is undesirable in cane sugar crystallization process. Generally, *D(4,3)* parameter is used to determine the crystal growth, which is obtained manually.

Specialized equipment for calculates the *D(4,3)* is available such as, microscopy, electro zone sensing and low angle laser light scattering, however these equipment's are very expensive

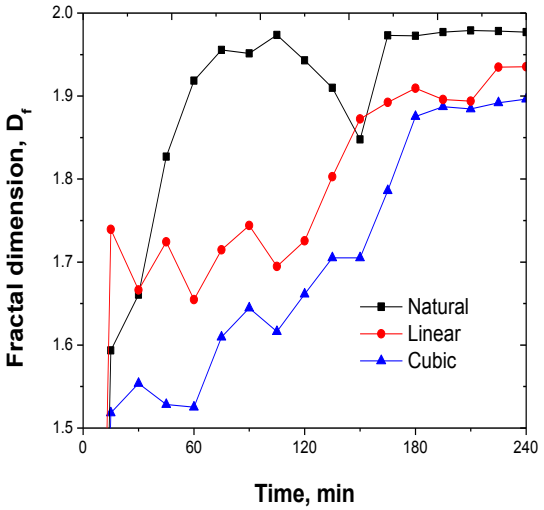

Fig. 7. Fractal dimension dynamic at different operation conditions

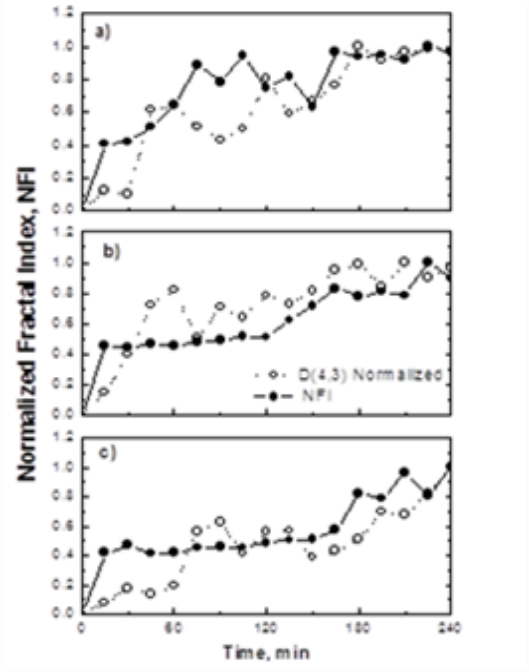

Fig. 8. Normalized fractal index versus crystal mean diameters, a) linear, b) natural and c) cubic temperature profiles

and difficult to implement insitu at the industrial level.

In this sense, it is necessary to develop more efficient methods for crystal monitoring [5,11,16]. A proposal can be quantifying of the number of pixels in the crystal images captured online during the crystallization process. For this, average pixels (P_A) calculation from binarized images is proposed.

Considering the three cooling profiles, Figure 5b shows the average pixels calculated by means of micrographs captured in periods of 15 min, where it can be seen that P_A is related to the crystals emergence, but it is not possible to distinguish if crystal presence is due to growth or nucleation. In addition, by adequate binarization of the image, the fractal analysis can provide an index, which can be correlated to crystal size. This parameter is qualitative, but can be used for indirect monitoring of crystals [14]. Using images at =60, 120, 180 and 240 min, Figure 6 shows the application of *R/S* analysis to cane sugar crystals images, where it is observed that scaling exponents exhibit dynamic variations for each temperature cooling profile, i.e., *R/S* analysis provide information about crystal growth.

In Figure 7 the average D_f values for three experiments is presented. Notice that, although the fractal dimension provides information about crystal formation, it is not possible to determine a direct correlation with *D(4,3)*. Complementing the obtained information, P_A from the binarization, and D_f from the fractal analysis, a mixed parameter is proposed that considers the information from both analyses. For such, the fractal dimension and average pixels are normalized as $\overline{D}_f = D_f / D_{f,max}$, and $\overline{P}_A = P_A / P_{A,max}$ where $D_{f,max}$ and $P_{A,max}$ are the highest values. Thus, the normalized fractal index is obtained as $NFI = \alpha \overline{D}_f + (1-\alpha)\overline{P}_A$, where $\alpha \in [0,1]$ is a constant value.

Figure 8 shows the comparison between *NFI* and *D(4,3)*, where it can be observed that for all cases the *NFI* satisfactorily adjusts the *D(4,3)* tendency.Calculating the Pearson correlation, a correlation degree is higher than 85% is obtained for all cases, which indicates that the *NFI* can be used as a parameter for indirect monitoring of crystals size growth in cane sugar production.

5 Conclusions

In this work, a combined method between *R/S* analysis and binarization images to analyze micrographs captured in pseudo-line for cane sugar crystallization process is proposed. Results indicate that fractal index can be used as an indirect monitoring variable, which allows tracking crystals size growth despite the cooling trajectory or supersaturation concentration implemented. Experimental tests to different operation conditions show direct correlations between normalized fractal index and *D(4,3)*, suggesting that the proposed methodology can be used for controlling and monitoring crystal growth.

References

1. **Eftekhari, A., Kazemzad, M., & Keyanpour-Rad, M. (2005).** Influence of atomic-scale irregularities in fractal analysis of electrode surfaces. *Appl. Surf. Sci.,* Vol. 239, No. 3, pp. 311–319. DOI: 10.1016/j.apsusc.2004.05.279.
2. **Zhang, B., Abbas, A., & Romagnoli, J. A. (2012).** Monitoring crystal growth based on image texture analysis using wavelet transformation. *IFAC P.* Vol. 45, No. 15, pp. 33–38.
3. **Damour, C., Benne, M., Boillereaux, L., Grondin-Perez, B., & Chabriat, J. P. (2010).** NMPC of an industrial crystallization process using model-based observers. *J. Ind. Eng. Chem.,* Vol. 16, No. 5, pp. 708–716. DOI: 10.1016/j.jiec.2010.07.014.
4. **Damour, C., Benne, M., Boillereaux, L., Grondin-Perez, B., & Chabriat, J. P. (2011).** Multivariable linearizing control of an industrial sugar crystallization process. *J. Process Contr.,* Vol. 21 No. 1, pp. 46–54. DOI: 10.1016/j.jprocont. 2010.10.002.
5. **Bolanos-Reynoso, E., Xaca-Xaca, O., Alvarez-Ramirez, J., & Lopez-Zamora, L. (2008**). Effect analysis from dynamic regulation of vacuum pressure in an adiabatic batch crystallizer using data and image acquisition*. Ind. Eng. Chem. Res.,* Vol. 47, No. 23, pp. 9426–9436. DOI: 10.1021/ie071594i.
6. **Pedreschi, F., Aguilera, J. M., & Brown, C. A. (2000).** Characterization of food surfaces using scale-sensitive fractal analysis. *J. Food Process Eng.,* Vol. 23, No. 2, pp. 127–143. DOI: 10.1111/j.1745-4530.2000.tb00507.x.
7. **Ismail, I. M. & Pfeifer, P. (1994).** Fractal analysis and surface roughness of nonporous carbon fibers and carbon blacks. *Langmuir,* Vol. 10, No. 5, pp. 1532–1538.
8. **Alvarez-Ramirez, J., Echeverria, J. C., & Rodriguez, E. (2008).** Performance of a high-dimensional R/S method for Hurst exponent estimation. *Physica A.,* Vol. 387, No. 26, pp. 6452–6462. DOI: 10.1016/j.physa.2008.08.014.
9. **De Anda, J. C., Wang, X. Z., & Roberts K. J. (2005).** Multi-scale segmentation image analysis for the in-process monitoring of particle shape with batch crystallisers. *Chem. Eng. Sci.,* Vol. 60, No. 4, pp. 1053–1065. DOI: 10.1016/j.ces.2004.09.068.
10. **Kaplan, L. M. (1999)**. Extended fractal analysis for texture classification and segmentation. *IEEE T. Image Process.,* Vol. 8, No. 11, pp. 1572–1585. DOI: 10.1109/83.799885.
11. **MasterSizer, S., Long Beb's User Manual (1997)**. Malvern Instruments. Ltd.: Westborough, MA.
12. **Bohlin, M. & Rasmuson, A. C. (1992).** Application of controlled cooling and seeding in batch crystallization. *Can. J. Chem. Eng.,* Vol. 70, No. 1 pp. 120–126. DOI: 10.1002/cjce.5450700117.
13. **Velazquez-Camilo, O. Bolanos-Reynoso, E., Rodriguez, E., & Alvarez-Ramirez J. (2010).** Characterization of cane sugar crystallization using image fractal analysis. *J. Food Eng.,* Vol. 100, No. 1, pp. 77–84. DOI: 10.1016/j.jfoodeng.2010.03.030.
14. **Velazquez-Camilo, O. Bolanos-Reynoso, E. Rodriguez, E., & Alvarez-Ramirez, J. (2010).** Fractal analysis of crystallization slurry images. *J. Cryst. Growth.,* Vol. 312, No. 6, pp. 842–850. DOI: 10.1016/j.jcrysgro.2009.12.060.
15. **Quintana-Hernandez, P., Bolanos-Reynoso, E., Miranda-Castro, B., & Salcedo-Estrada, L. (2004).** Mathematical modeling and kinetic parameter estimation in batch crystallization. *AIChE J.*, Vol. 50, No. 7, pp. 1407–1417. DOI: 10.1002/aic.10133.
16. **Rawle, A. (1999)**. Basic Principles of Particle Size Analysis (Technical Paper Ref. WR141AT; Malvern Instruments: U.K.
17. **Utrilla-Coello, R. G., Bello-Perez, L. A., Lara, V. H., Vernon-Carter, E. J., & Alvarez-Ramirez, J. (2014)**. A fractal analysis approach for predicting starch retrogradation from X-ray diffractograms. *Starch Starke,* Vol. 66, No. 1-2, pp. 166–174. DOI: 10.1002/star.201300040.
18. **Ţălu, Ş., Bramowicz, M., Kulesza, S., Solaymani, S., Shafikhani, A., Ghaderi, A., & Ahmadirad, M. (2016).** Gold nanoparticles embedded in carbon film: Micromorphology analysis. *J. Ind. Eng. Chem.,*

Vol. 35, pp. 158–166. DOI: 10.1016/j.jiec. 2015.12.029.

19. **Tahal, T. V. (2000).** New Models for Sugar Vacuum Pans. *Ph.D. Dissertation.*
20. **Sanchez-Ortiz, W., Andrade-Gómez, C., Hernandez-Martinez, E., & Puebla, H. (2015)**. Multifractal Hurst analysis for identification of corrosion type in AISI 304 stainless Steel. *Int. J. Electrochem. Sci.,* Vol. 10, pp. 1054–1064.
21. **Wang, X. Z., De Anda, J. C., & Roberts, K. J. (2007).** Real-Time Measurement of the Growth Rates of Individual Crystal Facets Using Imaging and Image Analysis: A Feasibility Study on Needle-shaped Crystals of L-Glutamic Acid*. Chem. Eng. Res. Des.,* Vol. 85, No. 7, pp. 921–927. DOI: 10.1205/cherd06203.

Article received on 12/05/2018; accepted on 15/07/2018. Corresponding autor is Armando Campos-Dominguez.